SUPPORTING INFORMATION

HALF HEDGEHOG SPIN-TEXTURES IN SUB-100 NM SOFT MAGNETIC NANODOTS

Eider Berganza[1,2]*, Miriam Jaafar[1,3]*, José Á. Fernández- Roldán[1,4], Maite Goiriena-Goikoetxea[5,6], Javier Pablo-Navarro[7], Alfredo García-Arribas[6,8], Konstantin Guslienko[9,10], César Magén[7,11,12], José M. de Teresa[7,11,12], Oksana Chubykalo-Fesenko[1] and Agustina Asenjo[1]

1 Instituto de Ciencia de Materiales de Madrid, CSIC, 28049 Madrid, Spain

2 Institute of Nanotechnology, KIT Campus North, 76344 Eggenstein-Leopoldshafen, Germany

3 Departamento de Física de la Materia Condensada and Condensed Matter Physics

Center (IFIMAC), Universidad Autónoma de Madrid, 28049 Madrid, Spain

4 Departamento de Física, Universidad de Oviedo, Federico García Lorca s/n, Oviedo 33007, Spain

5 Department of Electrical Engineering and Computer Science, University of California, Berkeley, CA 94720, USA.

6 Departamento de Electricidad y Electrónica, Universidad del País Vasco (UPV/EHU), 48940 Leioa, Spain.

7 Laboratorio de Microscopías Avanzadas (LMA) - Instituto de Nanociencia de Aragón (INA), Universidad de Zaragoza, 50018 Zaragoza, Spain.

8 Basque Center for Materials, Applications and Nanostructures (BCMaterials), UPV/EHU Science Park, 48940 Leioa, Spain.

9 Department of Materials Physics, University of the Basque Country (UPV/EHU), 20018 Donostia, Spain

10 IKERBASQUE, the Basque Foundation for Science, 48013 Bilbao, Spain

11 Instituto de Ciencia de Materiales de Aragón (ICMA), Universidad de Zaragoza-CSIC, 50009 Zaragoza, Spain.

12 Departamento de Física de la Materia Condensada, Universidad de Zaragoza, 50009 Zaragoza, Spain.

KEYWORDS Magnetic skyrmions, Magnetic Force Microscopy, Nanodots, Micromagnetism

*Corresponding authors: Eider Berganza, eider.eguiarte@kit.edu
Miriam Jaafar, miriam.jaafar@uam.es;

1: MORPHOLOGICAL AND STRUCTURAL CHARACTERIZATION

Two samples were fabricated by Hole-mask Colloidal Lithography. The first one, of 70 nm diameter and displaying a narrow size distribution (inset in Fig. S1a), was used to conduct the experiments presented in the manuscript. The second sample was later grown for a specific study addressed in section 7 of Supporting Information.

The size of the nanodots was assessed with SEM top view images, which allows performing a size distribution histogram. Furthermore, HRTEM was utilized to image the cross section of the nanodots and study their shape (Fig. S1b-e).

HR-TEM measurements evidence that the sample is polycrystalline. Since no preferential crystal orientation is found, it is confirmed that the sample does not possess net magnetocrystalline anisotropy.

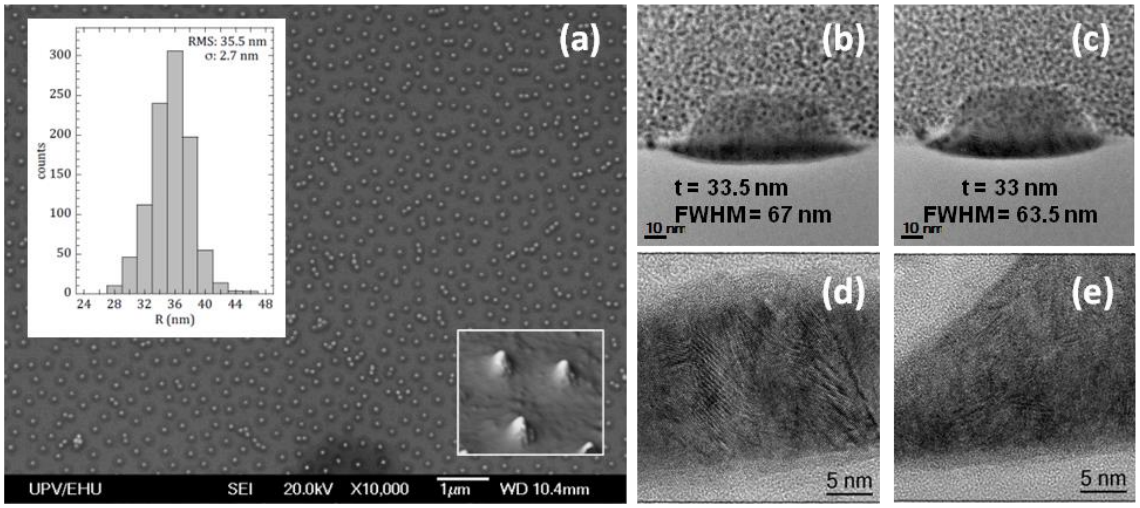

Fig. S1. (a) Scanning Electron Microscopy (SEM) top view image of sample A, with its corresponding size-distribution histogram and a 3D AFM topographic image in the insets (b) and (c) HR-TEM images of the cross section of typical dome-like shape nanodots of the sample A. (d) and (e) HRTEM images displaying the polycrystalline nature of the nanodots.

2: STUDY OF THE ELECTROSTATIC CONTRIBUTION TO THE FREQUENCY SHIFT (MFM CHANNEL)

To discard the presence of electrostatic and magnetic crosstalk, two different experiments have been conducted. On the one hand, Electrostatic Force Microscopy (EFM) tips have been utilized to image the sample, performing retrace at around 25 nm. The image (Fig. S2b) differs significantly from an equivalent image performed with the MFM tip (Fig. S2f) beyond the dark contrast in one upper edge. Additionally, when simultaneous the Kelvin Probe Force Microscopy (KPFM) mode is enabled to compensate the electrostatic interaction,[1] the signal is cancelled out in the frequency channel when the EFM tip is used (Fig. S2c), whereas with the magnetic tip, the image remains similar to the experiment with no Kelvin feedback. In both cases, the surface potential signal (shown in Figs. S2d and S2h) is mainly centred in the halo around the dots. Moreover, the contribution of the electrostatic interaction to the frequency shift (MFM channel) is around 10% on top of the nanodots probing that this electrostatic contribution is negligible compared to the magnetic one.

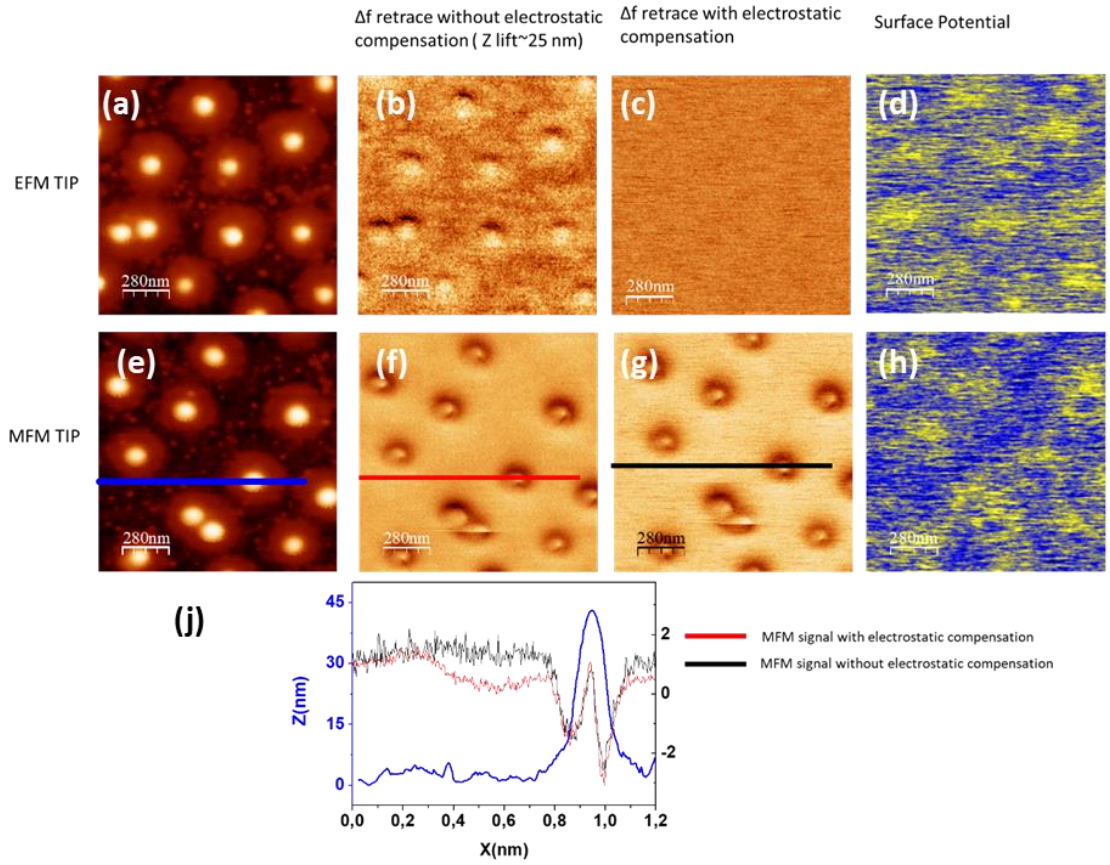

Fig. S2. Sequence of images obtained with (a)-(d) PtCr coated tips (EFM) and (e)-(h) MFM tips. Topography is shown in the first place, together with information from additional channels. In (b) and (f) the frequency channel is recorded without enabling simultaneous KPFM for the compensation of the electrostatic interaction. In the subsequent images (c)-(d) and (g)-(h) simultaneous MFM and KPFM modes are used, and the frequency channel is recorded, together with the surface potential. Notice that the electrostatic signal obtained using an EFM tip (Fig. S3 b) is not related with the typical MFM signal observed in our sample beyond the dark contrast in one upper edge. Moreover, the surface potential signal is mainly centered in the halo around the dots while the contribution of the surface potential to the frequency shift (MFM channel) is around 10% on top of the nanodots.

3: MFM DATA INTERPRETATION

Given that the MFM imaging was conceived as a surface characterization technique where the probe is mainly sensitive to the OOP component of the sample stray field, one needs to keep always in mind that different magnetic configurations might give rise to similar imaging output. In this regard, the addition of complementary measurements under applied field and corresponding micromagnetic simulations can be crucial for an accurate interpretation of the results.

Considering the four magnetic configurations stabilized in micromagnetic simulations (Figure 2 of the main manuscript), Fig.S3 presents a table that establishes the expected MFM contrast for all possible cases. Notice that all the experimental images arise with a bright core because the tip-vortex core interaction is always repulsive. If we compare the expected MFM signal sketches with the real experimental data displayed in Figure 2a and c in the main text, we can see that only cases 3 and 4 are compatible. Therefore, cases I and II can be discarded.

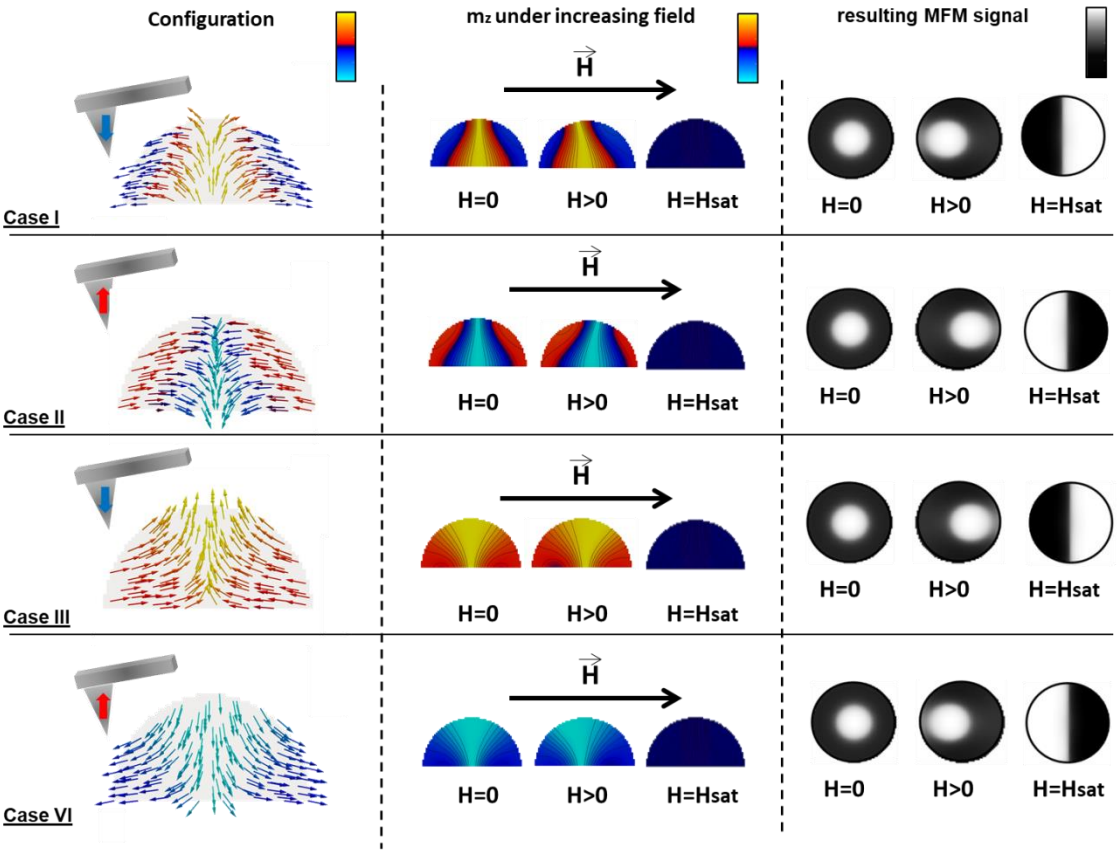

Fig. S3: The first column displays the 4 possible configurations that have been stabilized through micromagnetic simulation. The second column shows the corresponding evolution of the out-of-plane component of the magnetization under applied field of the configurations on the left. The corresponding sketches of the MFM bright-dark contrasts are shown on the third column.

4: TOPOLOGICAL CHARGE

In view of the strong dark-bright MFM contrast when analysing the contour and core intensities of the imaged nanodots, one might expect a configuration with certain topological charge.

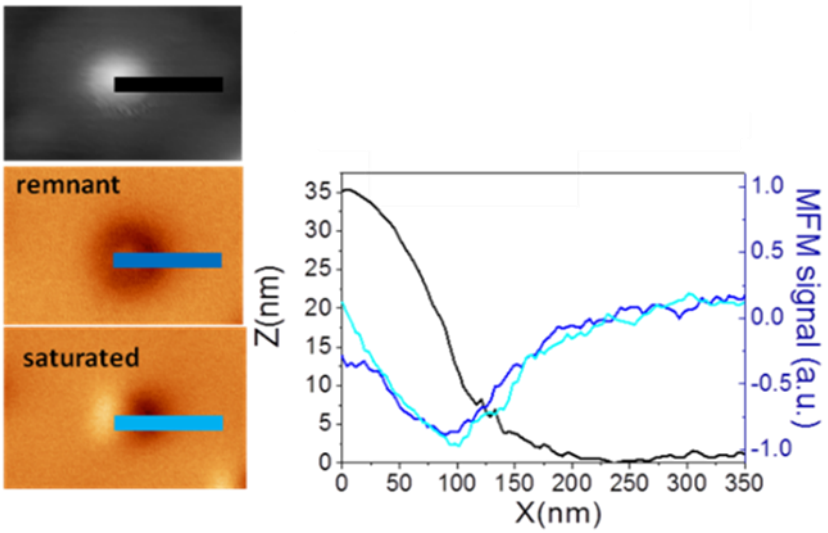

Fig. S4: Topographic and MFM images in remnant (dark blue) and nearly saturated states (light blue) of an imaged nanodot. Their corresponding normalized profiles are depicted on the graph.

In Figure S4, we compare the intensities of the same nanodot in remnant state (half hedgehog) and under saturating in-situ field (dipole). Notice that the MFM signals have been normalized for the sake of comparison. Both profiles resemble both in the shape and the intensity.

Nevertheless, the surprisingly high intensity displayed by the half-hedgehog is rather due to the generated strong OOP stray field components. As it is widely known, the MFM contrast is related to the force gradient experienced by the magnetic tip in the presence and as a result of the stray field of the sample.

5: IMAGING AT DIFFERENT HEIGHTS

Using a commercial MFM tip (type 1), a selected area of the sample was imaged at increasing retrace distances (Fig. S5). As a consequence, the contrast intensity is reduced and the core contrast expands slightly due to the bigger averaging at higher distances. Nevertheless, the sequence of profiles in Fig. S5i shows that the integrity of the configuration does not significantly change with the smaller tip stray influence.

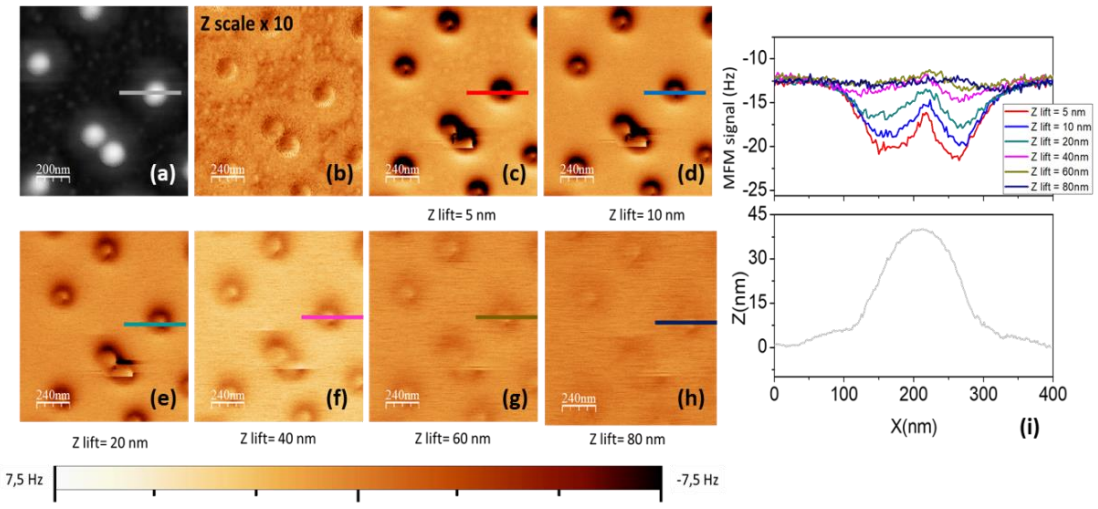

Fig. S5. (a) Topography and (b) frequency shift image obtained simultaneously (during the first scan) (c)-(h) MFM images of the same area of the sample obtained at different retrace distances. The corresponding profiles are plotted in (i), together with the topography profile.

6: DETERMINATION OF CRITICAL FIELDS AND TIP STRAY FIELD VALUES

The tip magnetic stray field can be tuned simply by controlling the amount of the magnetic coating (usually Co based layer) deposited.[2] To obtain probes with less stray fields, than commercial probes, a Co thin film was sputtered onto commercial AFM tips choosing the desired thickness, *i.e.* adjusting the local stray field. However, this method has some limitations; as the coating thickness decreases the MFM signal to noise ratio can be jeopardized. In this work, Fe nanorods were grown by Focused Electron Beam Induced Deposition (FEBID) on standard AFM tips.[3] Nanorod diameters below 35 nm with very sharp endings (7 nm) can be obtained to improve the lateral resolution and reduce even more the stray field. Moreover, the cylindrical geometry and the high aspect ratio of the Fe nanorods maximize the OOP vs. IP stray field ratio.

In this section, the methodology followed to obtain the half-hedgehog critical values is explained. Prior to the performance of advanced VF-MFM modes, a standard MFM image is obtained with the desired tip. This way, the magnetic core of a particular nanodot can be located. Next, the scan is stopped in the slow direction, and the diameter of the dot is repeatedly scanned (see the yellow line in Fig. S6a). A field sweep is enabled in the desired range and the magnetic image is recorded (so called the MFM based 3D mode). The resulting image (Fig. S6b) allows discriminating areas where the nanodot is nearly saturated (marked with a magenta brace) and the area where the half-hedgehog exists, namely its "mean life" field range, within the two dashed blue lines. This method also enables the visualization of the half-hedgehog core movement, nucleating in the right edge at -4 mT until it is annihilated in the left edge at 0 mT. The error of the measurements, coming from various sources, is estimated to be of 2 mT.

The critical fields show a clear dependence on the stray field arising from the MFM probe (Figure 5a,in the main text). Among the different methods to estimate the tip stray field, we have used a simple and practical method based on the calibration of a reference sample. A CoPt thin film with well-defined out-of-plane magnetization domains is imaged with each tip at their corresponding working distance (Fig. S6c). Profiles of each image are plotted to extract the maximum MFM signal (frequency shift) for each tip, as in Fig. S6d. These values are correlated to the force gradient values as explained in the methods section. Assuming that the sample magnetization remains constant, the force gradient is proportional to the tip stray field.

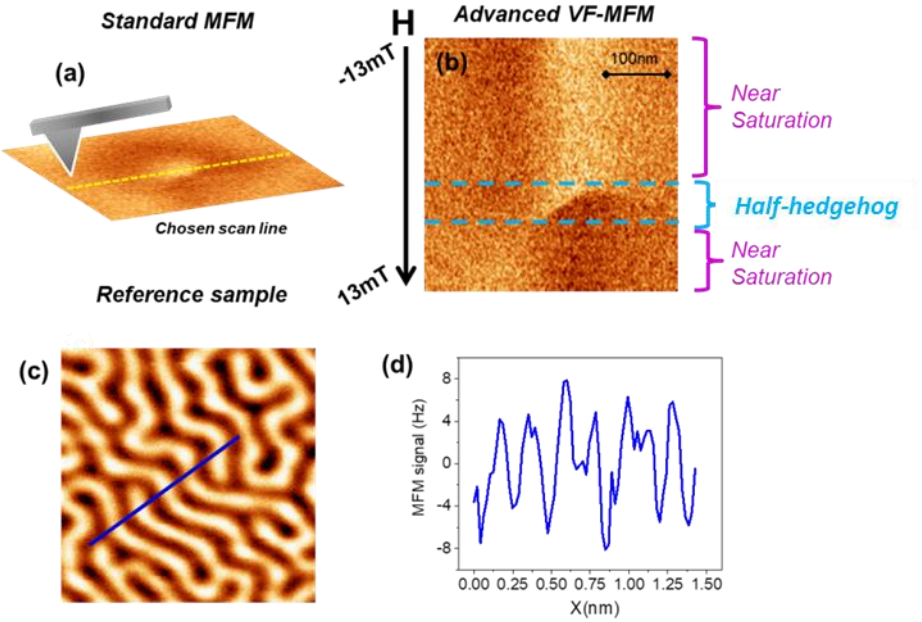

Fig. S6. (a) Standard MFM image of the nanodot to localize the half-hedgehog core. (b) Advanced VF-MFM measurement. The yellow line in (a) is repeatedly scanned, while the field is varied. The nearly saturated areas at the top and bottom of the image are marked by magenta colour. In the central area the half-skyrmion exists (marked in blue) within the dashed blue boundaries. (c) MFM image of the reference sample with well-defined OOP domains of homogeneous stray field intensity. (d) The profile from (c) used to extract the maximum magnetic signal value obtainable for each different tip.

On the other hand, the out-of-plane signal of the tips was evaluated with a reference sample. The output, obtained in Hz after enabling the PLL, was correlated to the magnetic force gradient through the following formula:

$$\Delta\omega \approx -\frac{\omega_0}{2k}\frac{dF_{t-s}}{dz},$$

where k is the cantilever force constant and Fs-t is the force experienced by the tip as a result of the stray field of the sample.

7: INFLUENCE OF GEOMETRICAL PARAMETERS

A sample with smaller nanodot diameter (60 nm in average) was fabricated, hereafter referred as B, with the objective of conducting an experimental study on nanodots with slightly smaller diameters. Sample B was therefore fabricated through HCL starting with smaller polystyrene spheres. A SEM image of sample B and the calculated size distribution histogram is presented in Supporting Information 7. Notice that the size distribution of sample B (σ = 3.4 nm) is wider than the distribution of sample A (σ = 2.7 nm). This fact can give us a further insight on the magnetic configurations. Since the radial component of the tip stray field stabilizes the half-hedgehog configuration, the lowest interacting tip obtained through FEBID was utilized for MFM imaging.

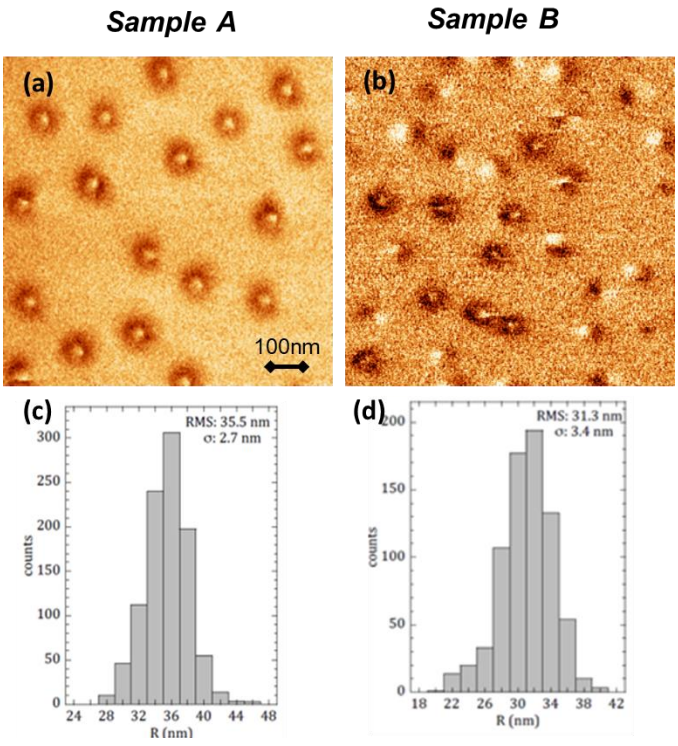

Fig. S7: (a) and (b) present MFM images of samples A and B respectively, scanned with a low moment tip. Below the corresponding size dispersion diagram of each sample can be found in (c) and (d).

The MFM image of Sample A (Figure S7a) shows 100% of half-skyrmion configurations in spite of the imaging with a low interacting tip. Further images were performed to enrich the statistics and no variation was found. The magnetic image of Sample B presents nonetheless a

different trend. Black-white dipolar contrasts are indicative of in-plane configurations (Fig. S7b). We note that since the sample is demagnetized (similar to Sample A), the dipoles show different orientations. After various images were taken in different sample areas, we can claim that half-skyrmions constitute around 22% of the configurations, while 66% of single domain configurations are present.

The remaining 12% correspond to ambiguous or changing configurations. Although this research line remains open for deeper experimental studies, experimental evidence points at the existence of a lower radius boundary for the stabilization of half-hedgehog.

References

[1] Jaafar, M.; Iglesias-Freire, O.; Serrano-Ramón, L.; Ibarra, M. R.; de Teresa, J. M.; Asenjo, A. Beilstein J. Nanotechnol. 2011, **2**, 552–560.

[2] Iglesias-Freire, Ó.; Jaafar, M.; Berganza, E.; Asenjo, A. Beilstein J. Nanotechnol. 2016, **7**, 1068–1074.

[3] Pablo-Navarro, J.; Magén, C.; De Teresa, J. M. Nanotechnology 2016, **27** (28)